MULTI-CHANNEL ICE PENETRATING RADAR TRAVERSE FOR ESTIMATES OF FIRN DENSITY IN THE PERCOLATION ZONE, WESTERN GREENLAND ICE SHEET

Tate Meehan[1], John Bradford[1], H.P. Marshall[1], Erich Osterberg[2], Bob Hawley[2], Thomas Overly[2], Gabe Lewis[2], Karina Graeter[2], and Forrest McCarthy[3]

ABSTRACT

To better predict the response of the Greenland Ice Sheet (GrIS) to future warming, leading edge Regional Climate Models (RCM) must be calibrated with in situ measurements of recent snow accumulation and ablation. Mass balance estimates averaged across the entire Greenland Ice Sheet (GrIS) vary between models by more than 30 percent, and regional comparisons of mass balance reconstructions in Greenland vary by 100 percent or more. Greenland Traverse for Accumulation and Climate Studies (GreenTrACS) is a multi-year and multi-disciplinary science traverse in the western percolation zone of GrIS. During spring 2016, we used multi-channel 500MHz radar in a multi-offset configuration to survey more than 800 km from Raven Camp towards Summit Station. Multi-offset radar measurements can provide high precision electromagnetic (EM) velocity estimates of the firn to within ±0.003 m/ns. EM velocity, in turn, can be used to estimate firn density. Using the CRIM equation we estimate the average firn density to a depth of ~25 meters. Preliminary radar-derived average density estimates agree with cumulative average density estimates from a firn core measurement (~40 kg.m-3), despite the spatial heterogeneity of the firn. (KEYWORDS: multi-offset, GPR, Greenland, Ice Sheet, GreenTrACS, firn, density)

INTRODUCTION

Greenland Traverse for Accumulation and Climate Studies (GreenTrACS) incorporates the following scientific disciplines to study recent changes in the surface mass balance (SMB) of the Greenland Ice Sheet (GrIS): snow and ice physics, englacial geophysical imaging, geochemistry, and Weather Research and Forecasting (WRF) computational modeling. Surface mass balance is the summation of mass gains (snow accumulation) and mass losses (surface melting, sublimation/evaporation, and runoff) from the surface of an ice sheet. When compared to the other five regions, western Greenland displayed the largest regional acceleration in mass loss from 2002-2010 (Sasgen et al., 2012). Since 2005 accelerated mass loss is primarily due to SMB and secondarily due to ice discharge (Van den Broeke et al., 2009).

SMB is commonly estimated at regional scales using high-resolution regional climate models (Box, 2013), which rely on data reanalysis (Chen et al., 2009). For GrIS, climate data pooled during reanalysis are sparse and relies heavily on outdated accumulation measurements of the 1997-1998 Program for Arctic Regional Climate Assessment campaign (Van der Veen, 2003). GreenTrACS will provide much needed updates to the reanalysis consortium to lessen the disparage of wildly variable RCMs. In situ firn core and snow pit observations provide water equivalent and depth-age relationships essential for monitoring accumulation rates.

The multi-offset radar is applied to map firn stratigraphy and estimate firn density. When combined with firn core depth-age scales, analysis of the radar data provides a means to assess the past ~20-40 years of accumulation, surface melt and refreeze, and current meltwater storage residing within potential englacial aquifers. The acquisition and processing methods are an adaptation of the seismic imaging problem. Estimation of snow density and accumulation requires EM velocity analysis. Methods are discussed within the following section.

METHODS

Core 7 Study Site

At 2455 mAMSL core site 7 is the highest elevation site occupied during the 2016 GreenTrACS campaign. The firn densification is compaction driven at this elevation. We have selected the high elevation site as a starting

Paper presented Western Snow Conference 2017
Corresponding Author: Tate Meehan, tatemeehan@boisestate.edu, 1910 University Dr. Boise, ID, 83725
[1] Boise State University, Department of Geosciences
[2] Dartmouth College, Department of Earth Science
[3] Winter Wildlands Alliance

point for this analysis, as we expect less vertical and lateral variability in the electromagnetic wave field. The discussion is held to a ~1 km transect which passes directly through the firn core location. We plan to improve and produce this analysis for the entire length of the traverse.

Multi-offset Radar Data Acquisition

By towing an array of antennae at multiple prefixed offsets, radar traces are acquired as continually spaced common midpoint (CMP) gathers. This acquisition strategy allows for independent estimation of the EM velocity along the traverse route. EM velocity is leveraged to quantify physical properties of the firn. The trade-off between sample intervals in time and space, and the two-way recording time window is optimized. Operation of the multi-channel radar does not exceed 10 km/h (Figure 1).

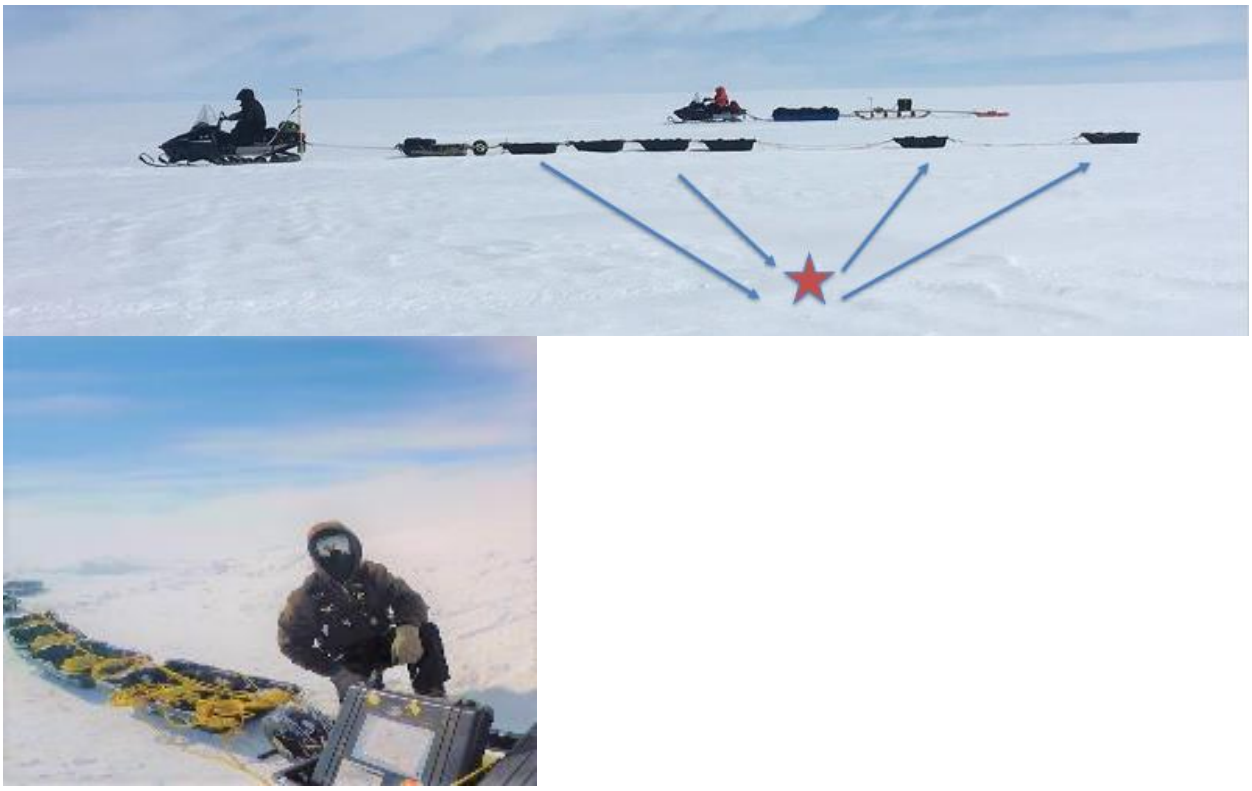

Figure 1. The multi-offset radar in operation (top) and under repair (bottom) during the 2016 GreenTrACS campaign. The star (top) represents the CMP location

Three transmitting (Tx) antennae and three receiving (Rx) antennae form nine independent Tx-Rx pairs. Antennae are separated linearly from 1.33 m to 12 m at far offset to capture the electric field response at a range of incidence (Table 1). A distribution of antenna separations is needed to accurately constrain the geometric relationship responsible for EM velocity analysis. As a rule of thumb the depth of investigation should approximately equal twice the longest offset.

Table 1. A channel is assigned a Tx-Rx pair with a horizontal separation. The channel is sequenced every 0.25 m while the radar is in tow. Channel assignments are clever to minimize the spatial bin width of a CMP gather.

Channel	**1**	**2**	**3**	**4**	**5**	**6**	**7**	**8**	**9**
Tx-Rx	1-1	1-2	1-3	2-1	2-2	2-3	3-1	3-2	3-3
Offset	4	8	12	2.67	6.67	10.67	1.33	5.33	9.33

The impulse wavelet is triggered by an odometer wheel coupled to the snow which sequences every 0.25 m. The recorded data are a multiplexed matrix with headers identifying the trace number and channel. The traces are de-multiplexed, sorted by offset and CMP location, and stored in matrices for further signal processing. The common midpoint interval is 2.25 meters and is equivalent to the distance traveled while the radar sequences through the 9 channels. The common midpoint location is the half difference of the channel offset plus the sequence position. The common midpoint bin is the 9 traces which most nearly occupy the same refection point within the firn and uniquely span the full range of offsets. The spatial width of the CMP bin is approximately half the midpoint interval.

Signal Processing

To remove unwanted signal, the de-multiplexed and sorted CMP gathers are band-pass filtered between 250 and 1000 MHz and reduced to a mean of zero. The traces are adjusted in time to remove systematic errors of the recorded two-way travel time. The time-zero correction is performed by automatic first break time-picking using the Modified Energy Ratio (MER) of Wong et al. (2009). The direct wave velocities corroborate with snow pit measurements of the surface density. The method for estimating snow density is described within the subsection Complex Refractive Index Method.

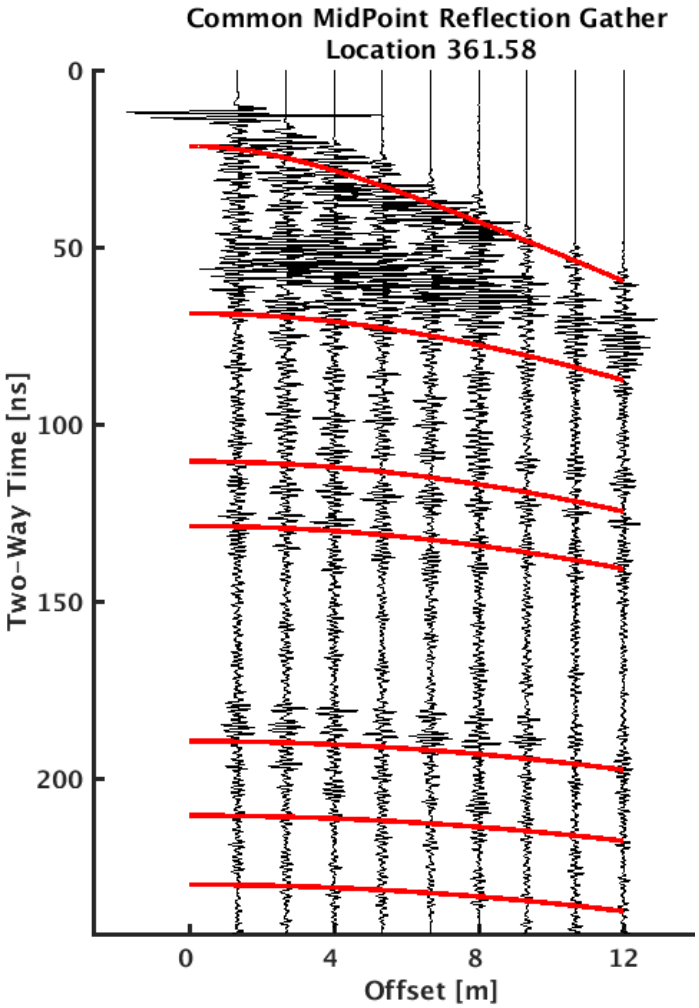

Figure 2. The processed CMP gather nearest to the Core 7 site. Coherent reflection horizons are represented by optimum trajectory curves. The depicted curvature expresses the firn velocity by the normal moveout equation.

Normal Moveout Velocity Analysis

The normal moveout equation (Equation 1) is the relationship among horizontal offset (x), the travel time (t_o) when x is zero, the root-mean squared subsurface velocity (V), and the recorded reflection travel time (t) at offset x.

$$t(x) \cong \sqrt{t_o^2 - \frac{x^2}{v^2}} \qquad [1]$$

The normal moveout (NMO) approximation is valid provided these underlying assumptions: reflection horizons have shallow dip ($\leq 10^{\circ}$), subsurface velocity is homogeneous between reflection horizons and/or does not vary dramatically vertically or horizontally, and the offset/depth ratio is not much less than ½ (Yilmaz, 2001). Travel times influenced by NMO maintain a hyperbolic trajectory, as depicted in Figure 2. Sensitivity of the offset/depth ratio is observable in the flattening of the trajectory slope in the later coherent horizons.

Automated Velocity Picking

Stratigraphic horizons in the firn are approximately flat lying. However, within the percolation zone, it is likely stark velocity discontinuities, such as ice lenses and layers, exist. Abiding the assumptions of NMO, we apply normal moveout velocity analysis to estimate the RMS average firn velocity structure.

Velocity analysis was computed using a spectral velocity coherency measure (Neidell and Taner, 1971). The spectrum of EM velocities from 0.1689 to 0.245 m/ns span the physical spectrum of pure ice to low density snow in the dry regime (Ulaby et al., 1986). Spectral velocity analysis is conducted by scanning the range of possible velocities at all times and supplying this information into the NMO equation. All possible trajectories are plotted over the CMP data. The coherent reflection event of the velocity that increases the normalized summed energy above the threshold of 0.5 is selected via Monte Carlo simulation for each CMP gather (Booth et al., 2011). The velocity picks are then inverted into density estimates as described within the following subsection.

Complex Refractive Index Method

The Complex Refractive Index Method (CRIM) equation is a dielectric mixing formula used to determine the fraction of pore space within a medium (Rodriguez and Abreu, 1990). The measured electromagnetic velocity (V) is a function of the relative dielectric permittivity (ε) and velocity of electromagnetic radiation in a vacuum (c) (Equation 2).

$$V = \frac{c}{\sqrt{\epsilon}} \qquad [2]$$

Figure 3 depicts the linear mapping of EM velocity to firn density. The CRIM equation and physical constants are inscribed. Data of this study were collected during late spring with surface temperatures below freezing. Surface meltwater infiltration was not observed. Therefore, the CRIM equation applied consists of an ice matrix with pore fluid of air (Annan et al., 1994). The results of the velocity analysis and CRIM formulation are presented in the following section.

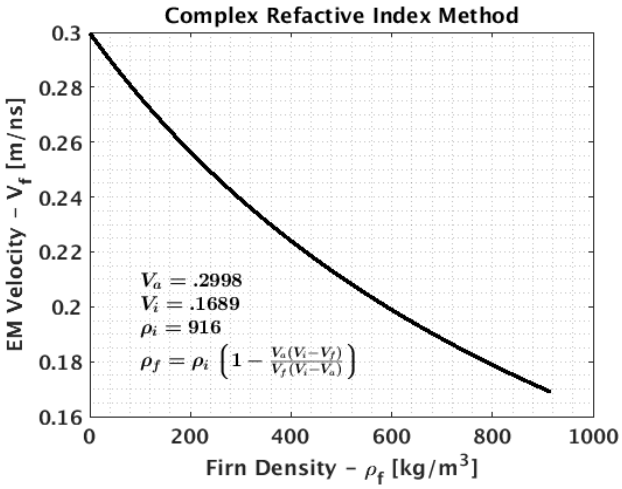

Figure 3. The CRIM velocity model is a linear relationship which maps the measured EM velocity to firn density. Subscripts *a*, *i*, and *f* denote contributions of air, ice, and firn.

RESULTS AND DISCUSSION

Velocity estimates from CMP gathers nearest the firn core are represented directly as estimates of cumulative average density and snow water equivalent via the CRIM equation (Figure 4). The scattered estimates overlay an interpolated estimate and measurements of the extracted core. Time to depth conversion has been performed using the RMS velocity. The smooth estimate is performed by a non-parametric moving weighted mean. The bi-squared kernel applies weights in a Gaussian form. And the window size has been optimized to minimize the RMSE between the core log and the radar derived estimates. Random error in the measurements shows no correlation with distance from the core site. Therefore, all neighboring data is given the same horizontal weighting.

The practice of gathering density and water equivalent from neighboring CMPs and smoothing is repeated along the 1 km traverse (Figure 5). Using a non-parametric approach for interpolating the estimate is flexible to be applied at different elevations, routes, and core sites along the traverse. The core data was used select an appropriate window size, though this is primarily a noise reduction technique and a different window could be used if desired. To interpolate along the traverse, the lateral window size was increased to include 40 neighboring CMPs. The larger window provides consistent information in regions of the firn where fewer coherent reflections were recorded.

Estimates of the cumulative water equivalent are more accurate because of the first order relationship. The integration of density by depth acts to remove variance in density as a source of error in the estimation of water equivalent. Long scale lateral variability is observable in the cumulative average density transect. NMO velocity analysis is shown to be useful tool despite the limitations. As a first pass and automated approach this is an encouraging result.

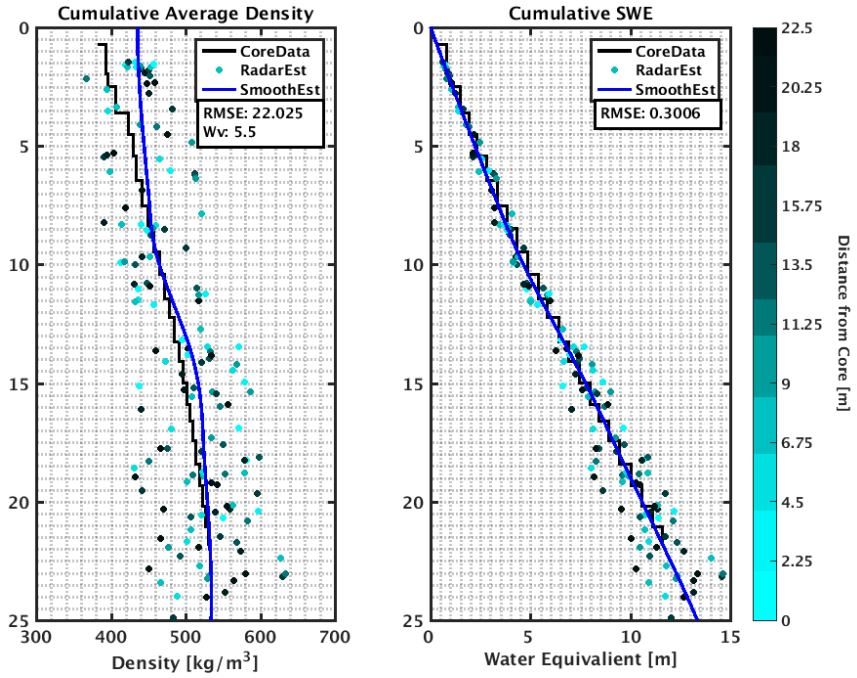

Figure 4. Cumulative average density (left) and water equivalent (right) estimates. Scattered points are derived by automated velocity analysis and CRIM. The smooth curve is the sliding weighted mean.

The future study is directed at estimating the snow accumulation rate. Multi-offset radar derived accumulation data can be placed on a decadal temporal scale by integrating the depth-age relation to coherent reflection horizons. The regional scale accumulation rate data can inform SMB influx and tune RCMs. 1 GHz multi-offset radar will complement the 500 MHz radar throughout the GreenTrACS 2017 campaign.

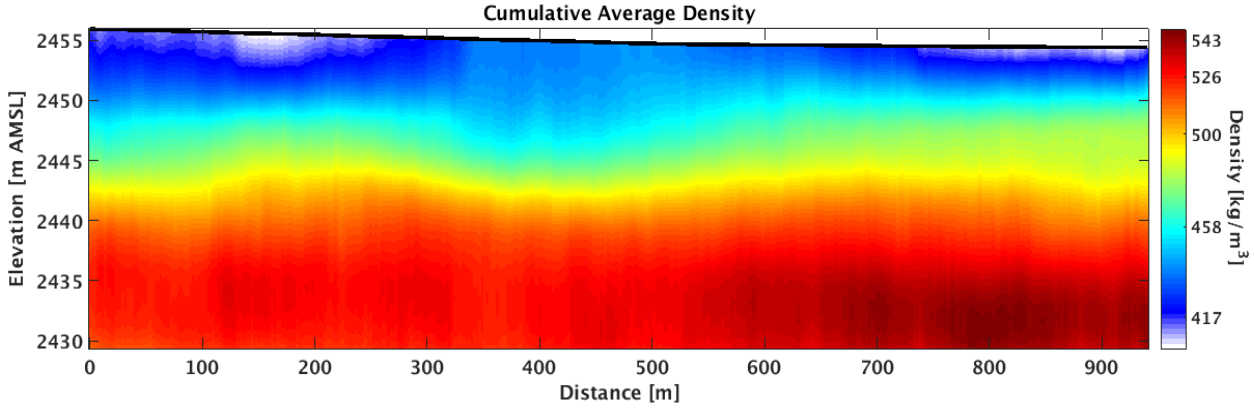

Figure 5. Cumulative average density expressed along the Core 7 transect. The EM velocity model reveals an intriguing and encouraging map of firn densification. The core site is nearest to location 361.5 m.

REFERENCES

Annan, A. P., S. W. Cosway, and T. Sigurdsson. 1994. GPR for snow pack water content. Fifth International Conference on Ground Penetrating Radar, 2.

Bindoff, N. L., J. Willebrand, V. Artale, A. Cazenave, J. M. Gregory, S. Gulev, K. Hanawa, C. LeQuere, S. Levitus, Y. Nojiri, C. K. Shum, L. D. Talley, and A.S. Unnikrishnan. 2007. Observations: oceanic climate change and sea level. In Climate Change 2007 The Physical Science Basis, vol. AR4, ISBN 9780521880, pp. 385–432.

Booth, A. D., R. A. Clark, and T. Murray. 2011. Influences on the resolution of GPR velocity analyses and a Monte Carlo simulation for establishing velocity precision. Near Surface Geophysics, 9(5), 399–411.

Box, J. E. 2013. Greenland ice sheet mass balance reconstruction. Part II: Surface mass balance (1840-2010). Journal of Climate, 26(18), 6974–6989.

Chen, L., O. M. Johannessen, H. Wang, A. Ohmura, and C. L. L. Chen. 2009. Accumulation over the Greenland Ice Sheet as represented in reanalysis data and related atmospheric circulation. 4(1), 11208.

Neidell, N. S. and M. T. Taner. 1971. Semblance and Other Coherency Measures for Multichannel Data. Geophysics, 36(3), 482–497.

Rogriguez, A. and R. Abreu. 1990. A Mixing Law to Model the Dielectrics Properties of Porous Media. Society of Petroleum Engineers.

Sasgen, I., M. van den Broeke, J. L. Bamber, E. Rignot, L. S. Sørensen, B. Wouters, Z. Martinec, I. Velicogna, and S. B. Simonsen. 2012. Timing and origin of recent regional ice-mass loss in Greenland.

Ulaby, F. T., R. K. Moore, and A. K. Fung. 1986. Microwave Remote Sensing: Active and Passive, vol. 3, Artech House.

Van den Broeke, M., J. L. Bamber, J. Ettema, E. J. Rignot, E. Schrama, W. Van de Berg, E. Van Meijgaard, I. Velicogna, and B. Wouters. 2009. Partitioning recent Greenland mass loss. Science, 326(2009), 984–986.

Van der Veen, C.J. (editor). 2003. Program for Arctic Regional Assessment (PARCA). Greenland Science and Planning Meeting, January 14-15, 2003, Byrd Polar Research Center, Columbus, Ohio. BPRC Technical Report No. 2003-02, Byrd Polar Research Center, The Ohio State University, Columbus, Ohio, pp. 56.

Wong, J., Han, L., Bancroft, J., and R. Stewart. 2009. Automatic time-picking of first arrivals on noisy microseismic data. CSEG Conference Abstracts.

Yilmaz, Oz. 2001. Seismic data analysis: processing, inversion, and interpretation of seismic data, Investigations in Geophysics no. 10, vol. 1, 2 ed., Society of Exploration Geophysicists.